Nonequilibrium kinetic phase transition of a monomer-dimer reaction model with sequential dimer adsorption in two dimensions

Da-yin Hua and Yu-qiang Ma*
National Laboratory of Solid State Microstructures, Nanjing University, Nanjing 210093, China
(Received 5 February 2002; published 4 September 2002)

We study a monomer-dimer reaction model in two dimensions in which the adsorption process of a dimer on the surface sites is separated into two steps (i.e., $B_2+*\rightarrow B_2*$, and $B_2*+*\rightarrow 2B*$, where * is an empty site), as first introduced by Evans and co-workers. It is clear that the dissociation of a dimer is dependent on the complicated configuration of the adsorbate. We show that the continuous transition from the reactive state to the O-passivated state and the discontinuous transition to the CO-passivated state both shift toward higher values of the fraction p of the monomer in gas phase but the reaction window decreases compared to the Ziff-Gulari-Barshad model. For the model studied here, the critical exponents of the continuous phase transition still exhibit a directed percolation character as expected.

DOI: 10.1103/PhysRevE.66.036101 PACS number(s): 05.70.Ln, 64.60.Ht, 82.65.+r

The study of the nonequilibrium phase transition in many particles system has attracted a great deal of interest over recent years, since they possess wide-ranging applications in many branches of physics, chemistry, biology, and even sociology [1]. Compared to their equilibrium cousin, the nonequilibrium phase transition is much less understood due to the lack of a general framework [1,2]. There is especially a substantial evidence in favor of the hypothesis that models in one dimension with a scalar order parameter exhibiting a continuous transition to a single absorbing state generally belong to the DP universality class. The directed percolation (DP) conjecture was first put forward by Grassberger and Janssen [3,4] and later extended by Grinstein, Lai, and Browne [5] to a multicomponent model in two dimensions. Moreover, Jensen and Dickman [6] have studied in depth two nonequilibrium systems in one dimension, which are shown to have the same critical behavior as the DP universality class again even if the continuous phase transition is from a reactive state into an inactive state with infinitely many absorbing states in these two models. The study of phase transitions for many nonequilibrium systems in one and two dimensions has shown that the critical behaviors of many models belong to the DP universality class, in spite of the quite dramatic differences in the microscopic processes of various models [1,2,6–13].

On the other hand, some works have shown that the additional symmetry and the conserved field are responsible for the new universality class of the critical behavior distinct from the DP universality [8,14–19]. More recently, the nonequilibrium phase transition in many systems has attracted a particular interest [2].

The nonequilibrium phase transitions occurring in the surface reaction models have attracted a great deal of interest since Ziff, Gulari, and Barshad (ZGB) first introduced a monomer-dimer model to describe the oxidation of carbon monoxide on a catalytic surface [20]. In their model, a monomer (CO) adsorbs onto a vacant site, while a dimer (O_2) adsorbs onto two adjacent vacant sites and dissociates. A nearest neighbor (NN) of a CO molecule and an O atom reacts and forms a CO_2 that desorbs from surface at once. In two dimensions, this model undergoes a continuous phase transition from the active reaction steady state into a unique O_2-poisoning state. This nonequilibrium continuous phase transition has been shown to be in the same universality class as the DP [5,21,22].

In the classical ZGB model, the complex sequence of intermediate steps of the adsorption of the dimer is neglected and a pair of NN sites for the dimer adsorbing trial is purely randomly selected in the simulation process. However, for an actual reaction on the surface, the adsorbing process of the dimer involves a very complicated dissociation on surface [23,24], and its dissociation depends on the surrounding chemical environment. Actually, Evans and co-workers [25,26] have first examined the influences of different dissociation processes of the dimer on the reaction system. On the other hand, Moiny and co-workers [27–29] have shown that the intrinsic adsorbate cluster on the heterogeneous catalytic reaction surface has an important effect on the reaction kinetics. Therefore, it is necessary to investigate the effect of the adsorbate cluster coupling with the complex process of the dissociation of the dimer on the phase transition of the ZGB model. In this paper, based on the model proposed by Nord and Evans [25], we show that the dissociation process of the dimer has a significant influence on the phase diagram of the reaction system but the critical behavior of the continuous phase transition remains unchanged.

In the model studied here, the monomer chemisorption is the same as the ZGB model, and the dimer adsorbing process incorporates the Langmuir-Hinshelwood mechanism in the appearance effect [30], i.e., $B_2+2*\rightarrow 2B*$, where * means an empty site. However, the microscopic process is separated into two steps [24–26]: (1) $B_2+*\rightarrow B_2*$; (2) $B_2*+*\rightarrow 2B*$. For the first step, a B_2 molecule adsorbs on one vacant site. Whether the adsorbed dimer dissociates continuously and how it occupies another site depend on its surrounding chemical environment. Obviously, whether the NN site is occupied or not should have different effects on the

*Author to whom correspondence should be addressed.

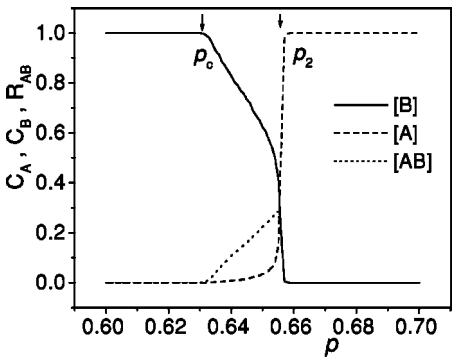

FIG. 1. The stationary state phase diagram showing three kinetic areas. The rate of AB production (R_{AB}) and the average coverage with A (C_A) and B (C_B) species are plotted as a function of p. Phase transitions occur at p_c and p_2.

dissociation of the adsorbed dimer. In order to simplify such an effect, we assume that the adsorbed dimer dissociates and randomly occupies a vacant NN site if there is at least one NN vacancy around it, otherwise, it desorbs at once. In the simulation process, the occupied NN site is avoided and only one of the NN vacant sites is randomly chosen for the second atom, which is effectively taken as a self-avoiding process. Therefore, the selection of a pair for the dimer adsorbing trial is no longer purely random because the configuration of the adsorbate on the catalytic surface significantly affects the selection.

The simulation process for the model of Nord and Evans [25] begins with a random collision of a gas molecule on a $L\times L$ square lattice with $L=256$. The colliding molecule is chosen to be a monomer (A) with a given probability p and a dimer (B_2) with a probability $1-p$. If the monomer A is chosen, the simulation steps are similar to these described in the classical ZGB model. If the dimer B_2 is selected, a site on the lattice is chosen randomly. If the site is occupied or the four NN sites are all occupied, the trial ends. Otherwise, a vacant site in the NN sites is selected randomly and the dimer adsorbs on the two sites. Furthermore, the adsorbing B atom reacts with an adjacent A to form a reactive product which desorbs at once and leaves two vacant sites.

By running static Monte Carlo simulation, we can find the general phase diagram. The system can be characterized by the fraction p of the monomer in gas phase. We see from Fig. 1 that the system has three different kinetic areas: when $p<p_c$, the system is passivated by the dimer atom, when $p>p_2(0.655\pm0.003)$ [20], the system is in the monomer-passivated state, and for p values between p_c and p_2 the system is in a reactive state. As p increases, we see that the system exhibits a continuous phase transition from the dimer-passivated state to the active state and then a discontinuous phase transition to the monomer-covered state. In the model studied here, with the domain formation of the adsorbed species, which mainly are the dimer atoms in the active reaction window, the effect of the configuration emerges mainly along the interface of the domain and increases the growth of the dimer domain because the adsorbed dimer is forced outward to choose another vacant site if the dimer first adsorbs on a vacant site along the interface. Therefore, the adsorption probability of the dimer on surface increases and the two critical points shift toward higher values of p but the reaction window decreases.

Due to the critical slowing down and strong finite-size effects, it is quite difficult to directly estimate the accurate critical value p_c and corresponding critical behaviors at p_c [31]. In this work, we employ the finite-size scaling (FSS) method developed for the nonequilibrium continuous phase transition by Aukrust, Browne, and Webman [31] to estimate the critical point p_c, the order parameter exponent β, and other correlation length exponents.

The order parameter describing the absorbing phase transition is ρ ($\rho=1-\langle\rho_B\rangle$, where $\langle\rho_B\rangle$ is the coverage of B atom on surface in the steady state); it behaves as follows when p approaches the critical probability p_c:

$$\rho\propto(p-p_c)^{\beta}, \tag{1}$$

where β is the order parameter exponent, and the critical point p_c is accurately estimated by the FSS method. There is a characteristic length scale ξ and a time scale τ that diverge at the critical point as

$$\xi\propto|p-p_c|^{-\nu_\perp}, \tag{2}$$

and

$$\tau\propto|p-p_c|^{-\nu_\parallel}, \tag{3}$$

where $\nu_\perp(\nu_\parallel)$ is a correlation length exponent in the space (time) direction.

At criticality, various ensemble-averaged quantities depend on the system size L through the ratio L/ξ of the system size and the correlation length. Therefore, we can take the following scaling form for the order parameter $\rho(p,L)$ close to the critical point:

$$\rho(p,L)\propto L^{-\beta/\nu_\perp}f[(p-p_c)L^{1/\nu_\perp}], \tag{4}$$

so that, at p_c

$$\rho(p_c,L)\propto L^{-\beta/\nu_\perp}, \tag{5}$$

and the scaling function

$$f(x)\propto x^{\beta} \tag{6}$$

for large x. In the supercritical region ($p>p_c$), the order parameter $\rho(p,L)$ remains finite in the limit $L\to\infty$, but it decays faster than a power law in the subcritical region ($p<p_c$).

For the characteristic time τ, we can take the following finite-size scaling form in the vicinity of p_c:

$$\tau(p,L)\propto L^{z}h[(p_c-p)L^{1/\nu_\perp}], \tag{7}$$

where $z=\nu_\parallel/\nu_\perp$ is the usual dynamical exponent. At p_c we have

$$\tau(p_c,L)\propto L^{z}. \tag{8}$$

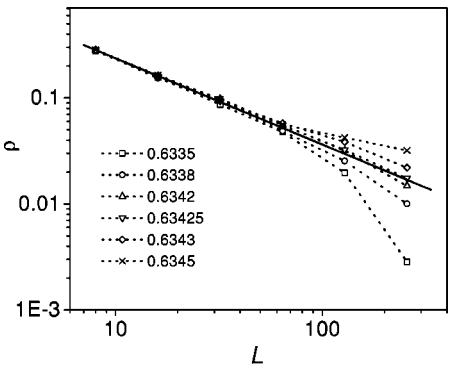

FIG. 2. The log-log plot for $\rho(p,L)$ versus L with different values of p. The slope of the straight line that goes through the data gives an estimate of the $-\beta/\nu_\perp$.

In order to measure the characteristic time τ, we calculate the moments τ_s for each sample s from an empty lattice until the poisoned state is reached

$$\tau_s(p,L,s)=\sum_t t\rho(p,L,t,s)/\sum_t \rho(p,L,t,s), \qquad (9)$$

where $\tau=\langle\tau_s\rangle_s$, and $\rho(p,L,t,s)$ is the order parameter defined above.

The Monte Carlo simulations are carried out with all sites vacated, and we use periodic boundary conditions. The system is allowed to change its configuration along the dynamic rules of the model studied here. A Monte Carlo step refers to an attempted adsorption on the average at every lattice site. The system first reaches a quasisteady state, stays for a reasonably long time, and finally evolves into an absorbing state. By measuring the concentration of the dimer in the quasisteady state and averaging over some independent samples which have not yet entered the absorbing state, we can get the order parameter ρ. In our simulation, to accurately measure the order parameter in the steady state, we first calculate the average of time sequences of the order parameter over a set of surviving independent trials until the end of the simulations, and then measure the stationary concentration from the time ensemble. The number of time steps ranges from 500 to 8×10^4. The number of independent surviving samples varies from 500 for the system size $L=8$ to 200 for $L=256$.

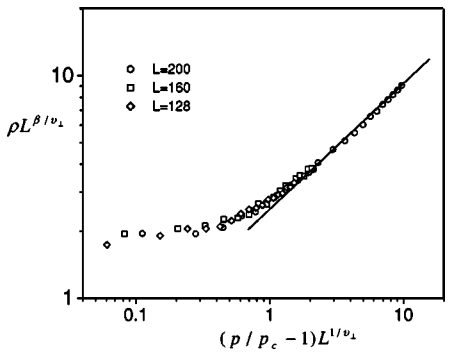

FIG. 3. The double-logarithmic plot for the data of $\rho L^{\beta/\nu_\perp}$ against $x=(p/p_c-1)L^{1/\nu_\perp}$ for various system sizes.

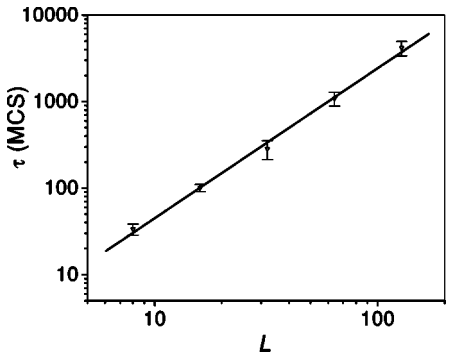

FIG. 4. The characteristic time against the system size L on a log-log plot. The solid line is of slope 1.73 $(=\nu_\parallel/\nu_\perp)$.

From Eq. (5), the data should fall on a straight line with a slope $-\beta/\nu_\perp$ for $p=p_c$ on a log-log plot of ρ as a function of L. In Fig. 2, we show the log-log plot of ρ as a function of L that is selected to be 8, 16, 32, 64, 128, and 256, respectively. We find $p_c=0.634\,25\pm0.000\,05$ (near the value 0.635 given by Ref. [25] and the value 0.633 in Ref. [26]), and $\beta/\nu_\perp=0.79\pm0.01$ at p_c from the slope of the straight line. This value of $\beta/\nu_\perp$ is in excellent agreement with that (0.80 ± 0.01) of the DP universality class [32], in contrast to the earlier result $(0.74\pm0.01$ at $p_c=0.387\pm0.001)$ of the classical ZGB model [5,33]. We can get further supporting results.

In Fig. 3, we have plotted $\rho L^{\beta/\nu_\perp}$ versus $x=(p/p_c-1)L^{1/\nu_\perp}$ on a log-log plot. From Eqs. (4) and (6), when x is small, the data should approach a constant, while for large x, the data should fall on a line with a slope β. It is shown that with the choices $\beta/\nu_\perp=0.79$ and $\nu_\perp=0.73$, the data for the various system sizes are well collapsed on a single curve. The solid line has a slope of 0.592 ± 0.007, which gives the asymptotic behavior for $\rho L^{\beta/\nu_\perp}$ as $L\to\infty$.

In Fig. 4, we show the characteristic time τ as a function of L on a log-log plot. From Eq. (8), the data should fall on a line with the slope $z=\nu_\parallel/\nu_\perp$ at the critical point. Every

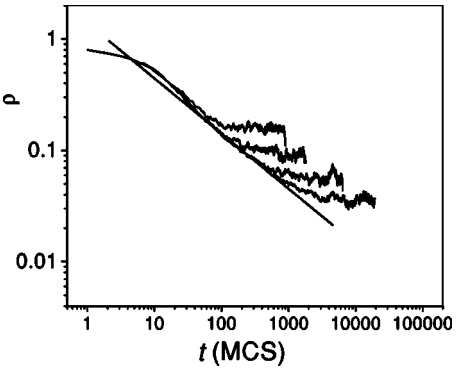

FIG. 5. The time dependence of the order parameter ρ for various sizes L at $p_c=0.634\,25$. From top to bottom, the curves correspond to $L=16$, 32, 64, and 128. The slope of the straight line gives the value of $\beta/\nu_\parallel(=0.45\pm0.04)$.

calculation result is averaged over 5000 samples, and we obtain the slope $z=1.73\pm0.06$ at $p_c=0.634\,25$. (For the original ZGB model, we find the result $z=1.69\pm0.06$.) This gives the value of $\nu_\parallel=1.26\pm0.06$ with the value $\nu_\perp=0.73\pm0.04$. To check our simulation results, we can also calculate the decay exponent of the order parameter at the critical point. For the time dependence of the order parameter $\rho(p_c,L,t)$ at criticality, one assumes a scaling form

$$\rho(p_c,L,t)\propto L^{-\beta/\nu_\perp} f(tL^{-\nu_\parallel/\nu_\perp}). \tag{10}$$

For $L\gg1$ and $t\ll L^{\nu_\parallel/\nu_\perp}$, we have the relation $\rho(p_c,L,t)\propto t^{-\beta/\nu_\parallel}$. In Fig. 5, we show the double-logarithmic plot of the $\rho(t)$ as a function of time t, and then we get $\beta/\nu_\parallel=0.45\pm0.04$, which is consistent with the above results.

In conclusion, we have discussed the effects of the dissociation process of the dimer coupling with the adsorbate clustering on the phase transition behavior of the ZGB model. In the Nord and Evans model, the configuration of the adsorbed species on the catalyst surface significantly affects the selection of a pair for the dimer adsorbing trial. The continuous transition points to the dimer-passivated state and the discontinuous transition points to the monomer-passivated state both shift toward higher values of p and the reaction window decreases. On the other hand, we compute the critical exponents of the continuous phase transition, which are $\beta=0.592\pm0.007$, $\beta/\nu_\perp=0.79\pm0.01$, $\beta/\nu_\parallel=0.45\pm0.04$, and $z=1.73\pm0.06$. This clearly indicates that in the model studied here, the continuous phase transition still shows a DP character [26,32]. The present study strongly indicates possibilities for examining the effects of the complex chemical environment at surface on the nonequilibrium phase transitions of chemical reaction systems, and checking the validity of the DP universality class in other multiatom reaction lattice-gas models due to differences in microscopic reaction details. We believe that further understanding will be highly desirable.

This work was supported by China's Outstanding Young Foundation under Grant No. 19925415, the National Natural Science Foundation of China under Grants No. 90103035 and No. 10021001, and the Trans-Century Training Program Foundation of the Talents by the State Education Commission.

[1] J. Marro and R. Dickman, *Nonequilibrium Phase Transitions in Lattice Models* (Cambridge University Press, Cambridge, England, 1999).
[2] H. Hinrichsen, Adv. Phys. **49**, 815 (2000), and references therein.
[3] H.K. Janssen, Z. Phys. B: Condens. Matter **42**, 151 (1981).
[4] P. Grassberger, Z. Phys. B: Condens. Matter **47**, 365 (1982).
[5] G. Grinstein, Z.W. Lai, and D.A. Brown, Phys. Rev. A **40**, 4820 (1989).
[6] I. Jensen and R. Dickman, Phys. Rev. E **48**, 1710 (1993).
[7] I. Jensen, Phys. Rev. E **47**, R1 (1993).
[8] H. Takayasu and A.Yu. Tretyakov, Phys. Rev. Lett. **68**, 3060 (1992).
[9] E.V. Albano, Phys. Rev. Lett. **69**, 656 (1992).
[10] E.V. Albano, J. Phys. A **29**, 3317 (1996).
[11] J. Zhuo and S. Redner, Phys. Rev. Lett. **70**, 2822 (1993).
[12] I. Jensen, Phys. Rev. Lett. **70**, 1465 (1993).
[13] P. Grassberger, J. Phys. A **22**, 3673 (1989).
[14] P. Grassberger, F. Krause, and T. von der Twer, J. Phys. A **17**, L105 (1984).
[15] P. Grassberger, J. Phys. A **22**, L1103 (1989).
[16] I. Jensen, J. Phys. A **26**, 3921 (1993); Phys. Rev. E **50**, 3623 (1994).
[17] N. Menyhard, J. Phys. A **27**, 6139 (1994).
[18] M.H. Kim and H. Park, Phys. Rev. Lett. **73**, 2579 (1994); Phys. Rev. E **52**, 5664 (1995).
[19] K.E. Bassler and D.A. Browne, Phys. Rev. Lett. **77**, 4094 (1996); Phys. Rev. E **55**, 5225 (1997).
[20] R.M. Ziff, E. Gulari, and Y. Barshad, Phys. Rev. Lett. **56**, 2553 (1986).
[21] C.A. Voigt and R.M. Ziff, Phys. Rev. E **56**, R6241 (1997).
[22] I. Jensen, H.C. Fogedby, and R. Dickman, Phys. Rev. A **41**, 3411 (1990).
[23] M.P. Harold and M.E. Garske, J. Low Temp. Phys. **127**, 553 (1991).
[24] P. Stoltze, Prog. Surf. Sci. **65**, 65 (2000).
[25] R.S. Nord and J.W. Evans, J. Chem. Phys. **93**, 8397 (1990).
[26] M. Tammaro and J.W. Evans, Phys. Rev. E **52**, 2310 (1995).
[27] F. Moiny and M. Dumont, J. Chem. Phys. **115**, 7705 (2001).
[28] F. Moiny, M. Dumont, and R. Dagonnier, J. Chem. Phys. **108**, 4572 (1998).
[29] F. Moiny and M. Dumont, J. Chem. Phys. **111**, 4743 (1999).
[30] T. Engel and G. Ertl, J. Chem. Phys. **78**, 2642 (1978).
[31] T. Aukrust, D. Browne, and I. Webman, Phys. Rev. A **41**, 5294 (1990).
[32] M.A. Munoz, R. Dickman, A. Vespignani, and S. Zapperi, Phys. Rev. E **59**, 6175 (1999).
[33] In the present simulation, we find the value $\beta/\nu_\perp=0.80\pm0.01$ by taking the critical value $p_c=0.387\,368\,2$ in Ref. [21] when the model of Nord and Evans is reduced to the classical ZGB model.